European Radiology (2019) 29:1375–1383
https://doi.org/10.1007/s00330-018-5673-y

HEAD AND NECK

Early white matter injuries associated with dopamine transporter dysfunction in patients with acute CO intoxication: A diffusion kurtosis imaging and Tc-99m TRODAT-1 SPECT study

Ming-Chung Chou[1,2,3] · Ping-Hong Lai[4,5] · Jie-Yuan Li[6,7,8]

Received: 13 May 2018 / Revised: 8 July 2018 / Accepted: 17 July 2018 / Published online: 24 August 2018

Abstract

Purpose Patients with CO intoxication were demonstrated to exhibit white matter (WM) injuries, changes in substantia nigra, dopamine transporter dysfunctions of striatum and Parkinsonism symptoms. We aimed to investigate the relationship between WM injuries of dopaminergic pathways and dopamine transporter dysfunctions of the striatum in patients with acute CO intoxication using both diffusion kurtosis imaging (DKI) and single photon-emission computed tomography (SPECT).

Materials and methods Seventeen patients with acute CO intoxication and 19 age- and gender-matched healthy subjects were enrolled. DKI data were acquired from all participants and Tc-99m-TRODAT-1 SPECT scan was performed on each patient. DKI datasets were fitted to obtain axial, radial and mean diffusivity, fractional anisotropy, axial, radial and mean kurtosis for voxel-based comparison. In addition, the TRODAT-1 binding ratio of the striatum was calculated using the occipital cortices as a reference. In significant regions, correlational analysis was performed to understand the relationship between DKI indices and TRODAT-1 binding ratio.

Results The results showed that DKI indices were significantly altered in multiple WM regions broadly involving the basal ganglia-thalamocortical circuit and nigrostriatal pathway. The correlation analysis further revealed significant correlations between DKI indices and the TRODAT-1 binding ratio in the nigrostriatal pathway (absolute correlation coefficients ranged from 0.5992 to 0.6950, $p<0.05$), suggesting that CO-induced early WM injuries were associated with dopamine transporter dysfunctions of striatum.

Conclusion We concluded that DKI and Tc-99m-TRODAT-1 SPECT scans were helpful in early detection of global WM injuries associated with dysfunctions of dopamine transporter in patients with acute CO intoxication.

Key Points

- *Voxel-based diffusion kurtosis imaging analysis was helpful in globally detecting early white matter injuries in patients with acute CO intoxication.*
- *CO-induced early white matter injuries were broadly located in basal ganglia-thalamocortical circuit and nigrostriatal pathway.*
- *Early white matter injuries in dopaminergic pathways were significantly correlated with dopamine transporter dysfunctions of the striatum.*

Electronic supplementary material The online version of this article (https://doi.org/10.1007/s00330-018-5673-y) contains supplementary material, which is available to authorized users.

✉ Jie-Yuan Li
jeffli2035@gmail.com

[1] Department of Medical Imaging and Radiological Sciences, Kaohsiung Medical University, Kaohsiung, Taiwan

[2] Department of Healthcare Administration and Medical Informatics, Kaohsiung Medical University, Kaohsiung, Taiwan

[3] Department of Medical Research, Kaohsiung Medical University Hospital, Kaohsiung, Taiwan

[4] Department of Radiology, Kaohsiung Veterans General Hospital, Kaohsiung, Taiwan

[5] Faculty of Medicine, School of Medicine, National Yang-Ming University, Taipei, Taiwan

[6] Department of Neurology, E-Da Hospital, No. 1, E-Da Road, Jiao-Su Village, Yan-Chao District, Kaohsiung City 824, Taiwan

[7] School of Medicine, I-Shou University, Kaohsiung, Taiwan

[8] Department of Nursing, Yuh-Ing Junior College of Health Care and Management, Kaohsiung, Taiwan

Keywords Diffusion magnetic resonance imaging · Carbon monoxide · Dopamine transporter

Abbreviations

ACR	Anterior corona radiata
AD	Axial diffusivity
AK	Axial kurtosis
BET	Brain extraction tool
CO	Carbon monoxide
COHb%	Carboxyhaemoglobin
CP	Cerebral peduncle;
DKE	Diffusion kurtosis estimator
DKI	Diffusion kurtosis imaging
DTI	Diffusion tensor imaging
FA	Fractional anisotropy
FSL	FMRIB software library
GCC	Genu of corpus callosum
GP	Globus pallidus
HBOT	Hyperbaric oxygen therapy
IC	Internal capsule
ILF	Inferior longitudinal fasciculus
MCP	Middle cerebellar peduncle
MD	Mean diffusivity
MK	Mean kurtosis
PCR	Posterior corona radiata
PLIC	Posterior limb of internal capsule
RD	Radial diffusivity
RK	Radial kurtosis
SCC	Splenium of corpus callosum
SCR	Superior corona radiata
SLF	Superior longitudinal fasciculus
SPECT	Single photon emission computed tomography
SPM 8	Statistical Parametric Mapping version 8
SS	Sagittal stratum
T_{coma}	Duration of coma
T_{onset}	Time after onset
WM	White matter

Introduction

Carbon monoxide (CO) intoxication represents an important issue in modern society. The inhalation of CO >100 ppm can gradually lead to unconsciousness and death. Patients who survive from CO intoxication usually exhibit neurological and psychological problems [1, 2]. Hyperbaric oxygen therapy (HBOT) was the mainstay approach to reduce neurological and psychological symptoms in unconscious CO intoxication patients [3], although the efficacy of HBOT remained controversial [4].

CO patients commonly showed white matter (WM) injuries, which led to neurological or psychological problems. In recent studies diffusion tensor imaging (DTI) was used to detect and characterize WM alterations in CO patients using axial (AD), radial (RD), mean diffusivity (MD) and fractional anisotropy (FA). Among them, AD and RD are the diffusivities measured in directions parallel and perpendicular to axons, respectively. MD is the averaged diffusivity of a diffusion tensor and FA is an indicator of tissue integrity [5]. It has been observed that the DTI indices were significantly altered in WM tissues and were associated with cognitive functions [6–9] and neuropsychological scores [6, 7, 9]. Moreover, diffusion kurtosis imaging (DKI) was demonstrated to be capable of estimating non-Gaussian water diffusion and can become an early biomarker of neurodegenerative process [10]. In DKI, axial (AK) and radial kurtosis (RK) are the measures of non-Gaussianity of water diffusion in directions parallel and perpendicular to axons, respectively, and mean kurtosis (MK) is the averaged diffusion kurtosis of a diffusion kurtosis tensor. A recent study performed tract-based DKI analysis in CO patients (within 8 days of intoxication) [11]. Results of this study demonstrated that DKI-related indices were more sensitive than DTI-related indices for the early detection of WM alterations caused by CO intoxication.

In addition, patients with CO intoxication frequently had globus pallidus (GP) lesions [6, 12, 13]. With the use of DTI and Tc-99m-TRODAT-1 single photon emission computed tomography (SPECT) scan, a previous study demonstrated that CO patients with Parkinsonian symptoms had significantly lower FA in WM tissues and a lower TRODAT-1 binding ratio in the striatum as compared to control subjects [6]. Results of this study suggested that pallidoreticular lesions were associated with poor cognitive functions, while dysfunctions of the globus pallidus (GP) and of the presynaptic dopamine transporter were related to Parkinsonian features. In addition, a previous study further demonstrated that substantia nigra was vulnerable to CO intoxication and changes in the substantia nigra were associated with CO-induced Parkinsonism [14]. As nigrostriatal pathway connects the substantia nigra and dorsal striatum, the WM alterations in the dopaminergic pathway may cause dysfunctions of dopamine transporter in striatum. Therefore, it is important to understand whether or not the early WM injuries are associated with the TRODAT-1 binding ratio, in order to institute early management of patients with acute CO intoxication.

In the present study we hypothesised that in patients with acute CO intoxication, WM injuries of dopaminergic pathways are associated with dysfunctions of dopamine transporter in the striatum. The purpose of this study was to investigate the relationship between WM alterations and dopamine transporter dysfunctions of the striatum in patients with acute CO intoxication using voxel-wise DKI analysis and Tc-99m-TRODAT-1 SPECT scan.

Methods

MRI data acquisition

The local institutional review board approved this study. Informed consent was obtained from each participant. Seventeen patients with acute CO intoxication and 19 age- and gender-matched healthy individuals with no history of neurological disease were enrolled in the study. The exclusion criteria were a history of major neurological and psychiatric disorders, pregnancy, metal implant and claustrophobia. Demographic characteristics of the subjects are shown in Table 1. Image acquisition was performed on a 1.5 T MR scanner (GE Healthcare, Milwaukee, WI, USA) using an 8-channel head coil. After a conventional T1-weighted (TR/TE=500/15 ms), T2-weighted (TR/TE=4200/96.7 ms) and FLAIR-weighted (TR/TE/TI=9000/128/2200 ms) images were acquired, whole-brain DKI data were acquired using a twice-refocused spin-echo diffusion-weighted pulse sequence characterised by the following parameters: TR/TE=10000/91 ms, b-values=1,000, 2,000 and 3,000 s/mm^2, number of b0 image=4, array coil spatial sensitivity encoding technique factor=2, number of diffusion directions=30, matrix size=80 × 80, field-of-view=240 × 240 mm, slice thickness=3 mm (isotropic), and number of excitation=1. The scan time for DKI acquisition was about 15 min.

Tc-99m-TRODAT-1 SPECT scan

In this study, SPECT scan was performed within 1 week prior to or following MRI examination. Before the SPECT scan, all patients were injected intravenously with 24 mCi Tc-99m-TRODAT-1 of contrast agent and followed by an uptake waiting period of 4 h. The TRODAT scan was performed on a SPECT/CT scanner (Symbia-T, Siemens) equipped with low-energy, high-resolution collimators and dual-slice spiral CT. First, spiral CT images were acquired using the following parameters: kVp=130 kV, current time product=17 mAs, slice thickness=5 mm. The images were reconstructed using an iterative filtered back-projection algorithm with a medium-smooth kernel. Second, the SPECT scan was performed using the following acquisition parameters:128 × 128 matrix size with 60 frames. The images were attenuation-corrected based on the CT images. The TRODAT-1 binding ratio of the striatum was obtained by calculating the ratio of the uptake in the striatum and occipital cortices using a previously published procedure [15]. The TRODAT-1 binding ratios of all CO patients are listed in Table 1.

Table 1 The demographic characteristics of enrolled carbon monoxide-intoxicated (CO) patients and healthy controls

	CO patients	Healthy controls
Gender (M/F)	8 / 9	10 / 9
Age (y/o)	41.5 ± 14.0	39.7 ± 11.6
Time after onset (days)	19.2 ± 11.0	N/A
Duration of coma (h)	25.6 ± 44.0	N/A
COHb%	25.0 ± 17.0	N/A
HBOT sessions	8.6 ± 5.0	N/A
Parkinsonian symptoms (M/F)	6 / 6	-
TRODAT-1 binding ratio	1.84 ± 0.31	-

CO carbon monoxide, *COHb* carboxyhemoglobin, *HBOT* hyperbaric oxygen therapy

Data processing

All DKI data were transferred to a stand-alone workstation and pre-processed offline using: FSL (FMRIB Software Library, Oxford University, Oxford, UK), DKE (Diffusion kurtosis estimator tool, NITRC), and SPM 8 (Statistical Parametric Mapping version 8, Wellcome Department of Cognitive Neurology, University College London, UK). First, the eddy-current distortions were corrected using a 12-parameter affine registration [16]. A brain mask obtained by BET (Brain Extraction Tool, FSL) was utilised to remove both scalp signal and background noise [17]. The DKI model was fitted on a voxel-by-voxel basis using DKE tool. Subsequently DTI-related indices, including AD, RD, MD and FA, and DKI-related indices, including AK, RK and MK, were obtained for comparisons. For voxel-based analysis, whole-brain FA maps were spatially normalised to an international consortium for brain mapping-FA template [18] using both linear affine and non-linear diffeomorphic demon registrations, respectively [19]. The displacement maps generated from the previous steps were utilised to spatially normalize the corresponding DKI maps.

The voxel-based analysis was performed using SPM8 to statistically compare all DKI indices between CO patients and healthy controls using a two-sample t test. The difference was considered significant with cluster-level corrected p value < 0.05 (uncorrected p<0.01 and cluster>100 voxels). The areas with significant difference were displayed as red-yellow colours superimposed on the averaged DKI maps. In CO patients, the correlation between DKI indices and time after onset (T_{onset}) may help to understand whether or not the WM injuries were progressed with time at early stage, and the correlation between DKI indices and duration of coma (T_{coma}) may help to understand the relationship between the severity of WM injuries and the severity of coma. Therefore, in significant regions, Pearson's correlation analysis was performed to reveal the associations between: DKI indices, T_{onset}, T_{coma}, carboxyhaemoglobin (COHb%) and TRODAT-1 binding ratio. The correlation was considered significant with a p value <0.05 and the correlation was considered moderate, strong and very strong if correlation coefficients ranged from 0.50–0.69, 0.70–0.89 and 0.90–1.0, respectively.

Results

In CO patients, AD was significantly higher than in control subjects, both in the bilateral fornix and in the right tapetum, as shown in Fig. 1. The MNI coordinates of regions with significantly different AD between the two groups are shown in Table S1. A significantly strong positive correlation was observed between AD and COHb% in the right tapetum (r=0.7274). However, no significant correlation was noted between AD, T_{onset}, T_{coma} and TRODAT-1 binding ratio in CO patients (see Online Supplementary Table S1).

A significant increase in RD was found in multiple WM areas in CO patients, including: bilateral Fminor, bilateral anterior corona radiata (ACR), bilateral sagittal stratum (SS), bilateral inferior longitudinal fasciculus (ILF), right thalamus, right GP, right superior longitudinal fasciculus (SLF) and genu of corpus callosum (GCC) (Fig. 1). The MNI coordinates of regions with significantly different RD between the two groups are shown in Online Supplementary Table S2. The correlation analysis revealed a moderate to strong positive correlation between RD and T_{onset} in the bilateral Fminor, left ACR, left SS and left ILF, and GCC (Table 2). On the contrary, a moderate negative correlation was observed between RD and TRODAT-1 binding ratio in the left SS (Table 3). However, no significant correlation was found between RD, T_{coma} and COHb% (Online Supplementary Table S2).

In CO patients, significantly increased MD was identified in multiple WM regions, including: bilateral Fminor, bilateral ACR, bilateral SS, bilateral ILF, right SLF and right GP (Fig. 1). The MNI coordinates of regions with significantly

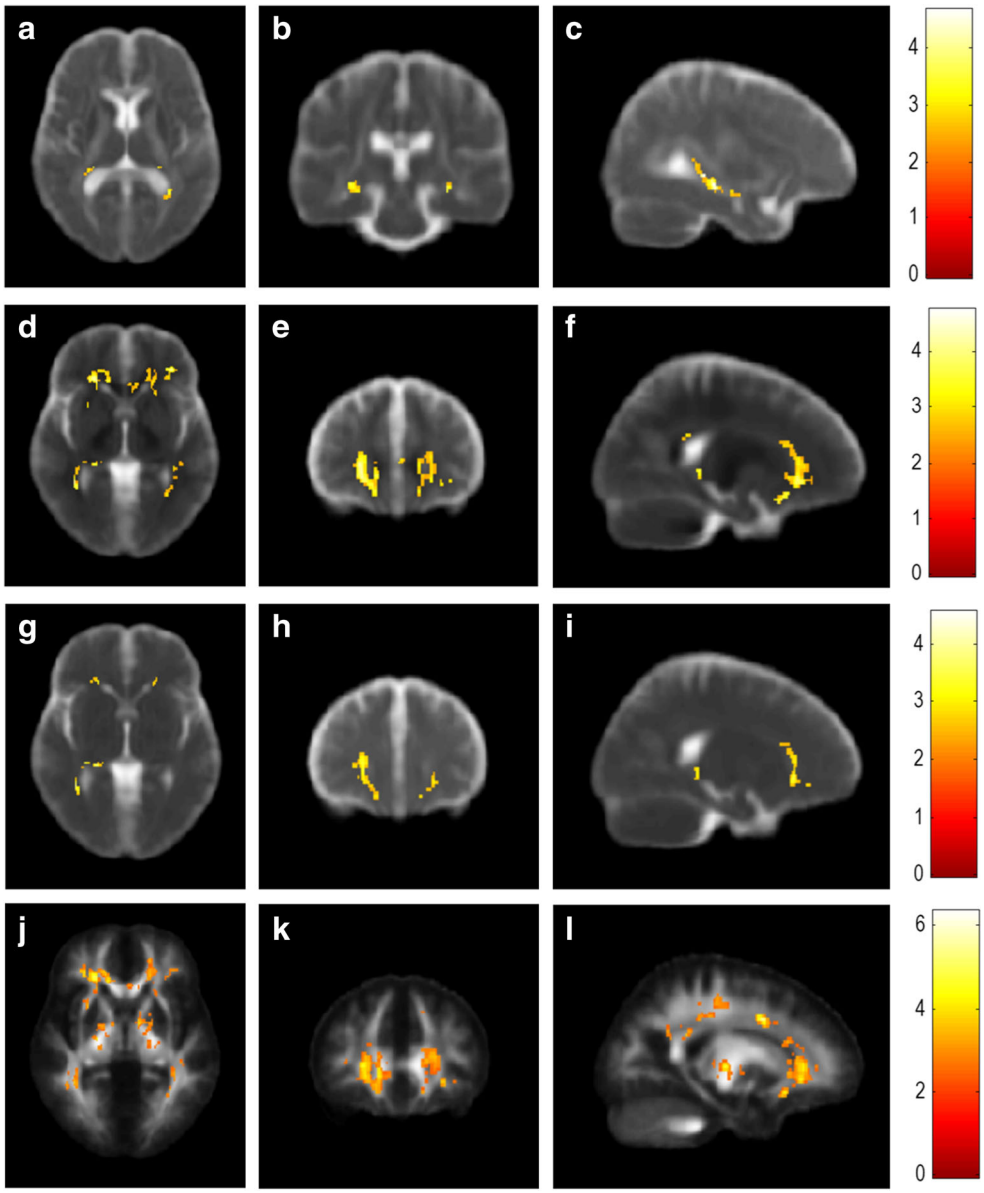

Fig. 1 Voxel-wise statistical comparisons of diffusion tensor-related indices between carbon monoxide-intoxicated patients and healthy controls. The regions with significantly increased axial diffusivity (top row; **a**, **b**, **c**), radial diffusivity (second row; **d**, **e**, **f**), mean diffusivity (third row; **g**, **h**, **i**) and significantly decreased fractional anisotropy (bottom row: **j**, **k**, **l**) are displayed in yellow-red colours superimposed on the corresponding averaged images

Table 2 Montreal Neurological Institute (MNI) coordinates of regions with significant correlation between the diffusion kurtosis imaging-derived indices and time after onset (T_{onset})

Brain region	MNI coordinate (mm)			Correlation coefficient
	X	Y	Z	
(RD and T_{onset})				
Rt. Fminor	17	35	-9	0.7270
Lt. Fminor	-16	35	-9	0.7435
Lt. ACR	-24	33	2	0.8051
Lt. SS	-36	-45	0	0.6670
GCC	7	26	4	0.7857
Lt. ILF	-36	-46	-2	0.7049
(MD and T_{onset})				
Lt. Fminor	-16	35	-9	0.6829
Lt. ACR	-24	33	2	0.5883
(FA and T_{onset})				
Rt. ACR	22	33	4	-0.5788
Lt. ACR	-22	33	4	-0.6650
GCC	-1	25	4	-0.6397
SCC	0	-30	19	-0.6151
Rt. CP	15	-20	-4	-0.5864
Rt. SS	37	-53	10	-0.6166
Lt. SS	-39	-46	8	-0.6517
(RK and T_{onset})				
Rt. Thalamus	10	-6	8	-0.6177
SCC	10	-36	22	-0.5694
Rt. PLIC	31	-27	16	-0.5940
(MK and T_{onset})				
Lt. Thalamus	-9	-12	6	-0.6181

RD radial diffusivity, *MD* mean diffusivity, *FA* fractional anisotropy, *RK* radial kurtosis, *MK* mean kurtosis, *ACR* anterior corona radiata, *SS* sagittal stratum, *GCC* genu of corpus callosum, *SCC* splenium of corpus callosum, *ILF* inferior longitudinal fasciculus, *CP* cerebral peduncle, *PLIC* posterior limb of internal capsule

different MD between the two groups are shown in Online Supplementary Table S3. Following a correlation analysis, a moderate positive correlation between MD and T_{onset} was revealed in the right Fminor and right ACR (Table 2), while a moderate negative correlation between MD and TRODAT-1 binding ratio was observed in the right GP (Table 3). However, no significant correlation was found between MD, T_{coma}, and COHb% (Online Supplementary Table S3).

FA was significantly decreased in several diffuse WM regions in CO patients. Major FA differences were found in the: GCC, splenium of corpus callosum (SCC), bilateral ACR, bilateral internal capsule (IC), bilateral SS, bilateral posterior corona radiata (PCR), right cerebral peduncle (CP) and right superior corona radiata (SCR) (Fig. 1). The MNI coordinates of regions with significantly different FA between the two groups are shown in Table S4. Following a correlation analysis, FA had

Table 3 Montreal Neurological Institute (MNI) coordinates of regions with significant correlation between the diffusion kurtosis imaging-derived indices and TRODAT-1 binding ratio

Brain regions	MNI coordinate (mm)			Correlation coefficient
	X	Y	Z	
(RD and TRODAT-1)				
Lt. SS	-36	-45	0	-0.6625
(MD and TRODAT-1)				
Rt. GP	16	3	-2	-0.6109
(FA and TRODAT-1)				
Rt. IC	13	-2	0	0.5992
(RK and TRODAT-1)				
Lt. PLIC	-24	-27	12	0.6882
(MK and TRODAT-1)				
Lt. PLIC	-24	-27	12	0.6950

RD radial diffusivity, *MD* mean diffusivity, *FA* fractional anisotropy, *RK* radial kurtosis, *MK* mean kurtosis, *SS* sagittal stratum, *GP* globus pallidus, *IC* internal capsule, *PLIC* posterior limb of internal capsule

a moderate negative correlation with T_{onset} in: GCC, SCC, bilateral ACR, right CP and right SS (Table 2). FA had a moderate to strong negative correlation with T_{coma} in: bilateral IC, right ACR, right SCR, and right CP (Table 4). Additionally, the correlation analysis also revealed a moderate positive correlation between FA and TRODAT-1 binding ratio in right IC (Table 3); however, no significant correlation was observed between FA and COHb% in CO patients (Online Supplementary Table S4).

Table 4 Montreal Neurological Institute (MNI) coordinates of regions with significant correlation between the diffusion kurtosis imaging-derived indices and duration of coma (T_{coma})

Brain regions	MNI Coordinate (mm)			Correlation Coefficient
	X	Y	Z	
(FA and T_{coma})				
Rt. ACR	22	33	4	-0.6220
Lt. IC	-13	-6	8	-0.7828
Rt. IC	13	-2	0	-0.5786
Rt. SCR	21	-25	41	-0.6680
Rt. CP	15	-20	-4	-0.6737
(RK and T_{coma})				
Rt. CP	13	-23	-4	-0.8333
Lt. CP	-18	-23	-4	-0.7284
Lt. PLIC	-24	-27	12	-0.6920
Rt. MCP	19	-46	-30	-0.5971
(MK and T_{coma})				
Rt. CP	18	-23	-4	-0.6547

FA fractional anisotropy, *RK* radial kurtosis, *MK* mean kurtosis, *ACR* anterior corona radiata, *IC* internal capsule, *SCR* superior corona radiata, *CP* cerebral peduncle, *PLIC* posterior limb of internal capsule, *MCP* middle cerebellar peduncle

AK was significantly lower in CO patients than in control subjects for the left fornix, as shown in Fig. 2. The MNI coordinates of regions with significantly different AK between the two groups are shown in Online Supplementary Table S5. No significant correlation was observed between AK, T_{onset}, T_{coma}, COHb% and TRODAT-1 binding ratio in CO patients (Online Supplementary Table S5).

In CO patients RK was significantly decreased in both supra- and infra-tentorial WM areas, including: bilateral ACR, bilateral CP, bilateral posterior limb of internal capsule (PLIC), right thalamus, right middle cerebellar peduncle (MCP) and SCC (Fig. 2). The MNI coordinates of regions with significantly different RK between the two groups are shown in Online Supplementary Table S6. Following a correlation analysis, a moderately negative correlation between RK and T_{onset} was observed in the right thalamus, right PLIC and SCC (Table 2). While a moderate positive correlation between RK and TRODAT-1 binding ratio was detected in left PLIC (Table 3). Moreover, a moderate-to-strong negative correlation between RK and T_{coma} was revealed in bilateral CP, left PLIC and right MCP (Table 4). However, no significant correlation was found between RK and COHb% in CO patients (Online Supplementary Table S6).

Significant increases in MK were also found in both supra- and infra-tentorial WM regions, including: bilateral CP, bilateral thalamus, bilateral PLIC, bilateral MCP and left ACR (Fig. 2). The MNI coordinates of regions with significantly different MK between the two groups are shown in Online Supplementary Table S7. The correlation analysis revealed a moderate negative correlation between MK and T_{onset} in the left thalamus (Table 2), and a moderate positive correlation between MK and TRODAT-1 binding ratio in the left PLIC (Table 3). Furthermore, a moderate negative correlation between MK and T_{coma} was also observed in the right CP (Table 4). However, no significant correlation was found between MK and COHb% in the patients (Online Supplementary Table S7).

Discussion

In this study, voxel-wise DKI analysis was performed in patients with acute CO intoxication with the aim of detecting global WM injuries. In CO patients, AD, RD and MD increased significantly, whereas FA, AK, RK and MK decreased significantly in multiple WM areas. Significant increases in AD, RD and MD and significant decreases in FA were observed in supratentorial WM. Our results are generally consistent with previous DTI findings [6–9, 11, 20–22]; however, in this study, decreases in RK and MK were also observed in both supra- and infra-

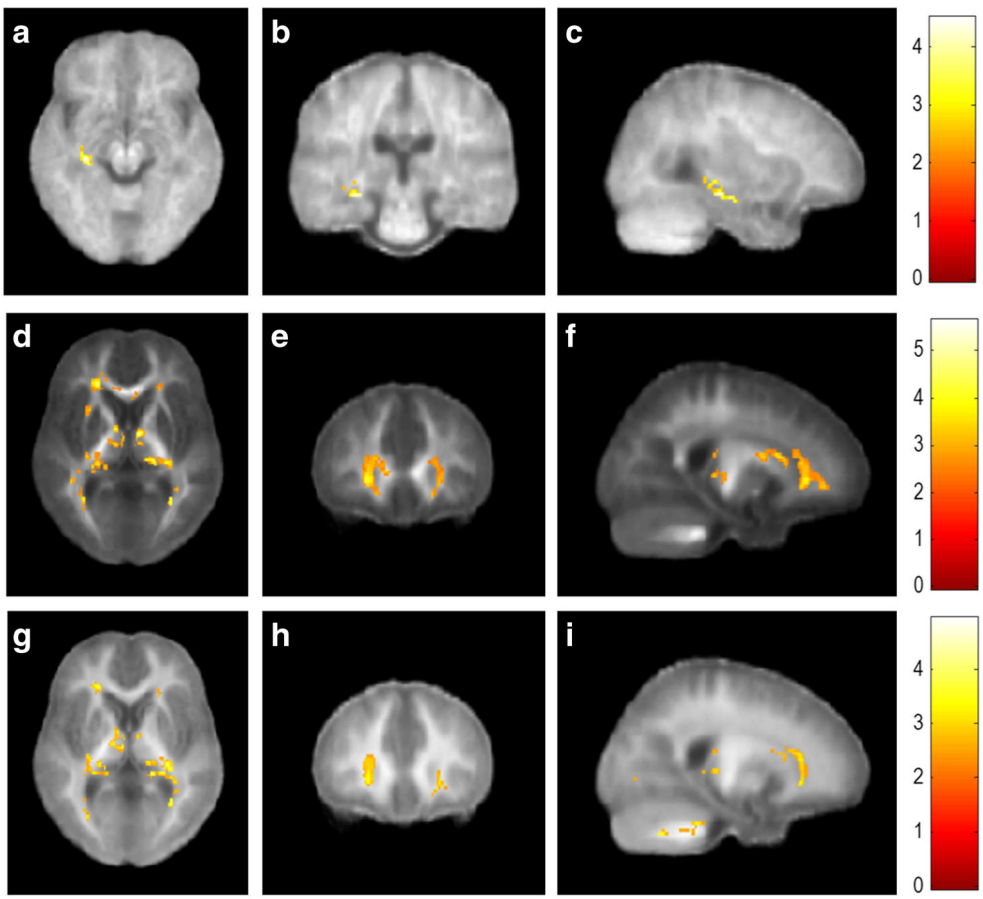

Fig. 2 Voxel-wise statistical comparisons of diffusion kurtosis-related indices between CO patients and healthy controls. The regions with significantly decreased axial kurtosis (top row; **a**, **b**, **c**), radial kurtosis (middle row; **d**, **e**, **f**) and mean kurtosis (bottom row; **g**, **h**, **i**) are displayed in yellow-red colours superimposed on the corresponding averaged images

tentorial WMs. A recent study performing tract-based DKI analysis on patients within 8 days post-CO intoxication found significantly decreased RK and MK in GCC, cingulum, corticospinal and corticobulbar tracts [11]. These observations were generally consistent with our results in supra-tentorial regions. This study further observed significantly decreased RK and MK in thalamus, CP, and MCP. Such results have not been mentioned in previous studies. Because RK and MK are the measures of non-Gaussian water diffusion and can reflect microstructural complexity of neuronal tissues [10], the results suggest that CO intoxication led to subtle changes in microstructural complexity at an acute stage that could be detected by DKI.

In CO patients, the right GP was found to exhibit significantly increased RD. Because GP plays an important role in the basal ganglia-thalamocortical circuit, the defective GP might be associated with Parkinsonism in the patients. A previous study demonstrated that CO patients with a GP lesion had a significantly lower TRODAT-1 binding ratio than those without a GP lesion at an average of 18 months post-CO intoxication [6]. In this study, similar findings were observed. Specifically, CO patients with a GP lesion had a lower Tc-99m TRODAT-1 binding ratio than those without a GP lesion (1.67 ± 0.35 vs. 1.92 ± 0.27), but the difference was not significant between them. In addition, the voxel-wise analysis also found that WM injuries were located near the: bilateral substantia nigra, bilateral thalamus, bilateral IC and bilateral corona radiata. These results suggest that CO intoxication partly damaged the basal ganglia-thalamocortical circuits and nigrostriatal systems and led to the symptom of Parkinsonism observed in CO patients at early stage.

Following a correlation analysis, this study showed that in critical regions, DKI indices were significantly correlated with T_{onset}, T_{coma}, COHb% and TRODAT-1 binding ratios to different extents. The injured WM regions had the most significant correlations between DKI indices and T_{onset}, suggestive of progressive WM alterations with time at acute stage. Hence, for those patients who exhibited no clinical symptom but early WM injuries, a series of HBOT may be considered to mitigate the progression of WM injuries and improve their prognosis. The DKI indices were significantly correlated with T_{coma} mainly in CP next to the substantia nigra, IC and MCP. It is known that consciousness is related to a brain arousal system the origin of which is the brainstem [23]. WM injuries of IC, CP and MCP were likely responsible for the duration of coma after CO exposure. These results suggested that for those comatose patients with more severe WM injuries, a series of more intensive HBOT may be considered to reduce WM injuries and the risk of cognitive sequelae. However, the level of COHb% in the blood was not significantly correlated with most WM injuries. This might be attributed to timing discrepancies between blood tests and MRI examinations (> 7 days) and HBOT treatment that has the effect of reducing the COHb% levels before the MRI scan. Interestingly, the DKI indices were significantly correlated with the TRODAT-1 binding ratio in GP, IC, PLIC and SS that broadly involved the nigrostriatal systems. Because the Tc-99m TRODAT-1 binding ratio is an indicator of dopamine transporter dysfunction, the WM injuries in those regions might be associated with the Parkinsonism observed in 12 CO patients. Therefore, for those patients who exhibited early WM injuries in dopaminergic pathways, care must be taken to monitor the signs and symptoms of Parkinsonism so as to implement early management of the symptoms and improve motor function and activities of daily living.

The pathophysiology of CO-induced early WM injuries associated with Parkinsonism remains unclear. In this study, WM injuries were detected mostly with increased RD and unchanged AD, suggestive of early WM demyelination at an acute stage [24]; however, caution must be exercised when interpreting changes to axial and radial diffusivities in regions with less organised WM bundles [25]. This study also shows significantly decreased FA indicating loss of WM integrity in CO intoxicated patients. In addition, diffusion kurtosis values that are a measure of non-Gaussianity of water diffusion can reflect microstructural complexity of brain tissue [10]. Our results demonstrate significant decreases in AK, RK and MK, suggesting an increased microstructural complexity in WM tissues caused by lipid peroxygenation [26] and production of reactive oxygen species [27], leading to reversible demyelinisation and neuronal necrosis after CO intoxication, respectively. Moreover, the early WM injuries were broadly located in the basal ganglia-thalamocortical circuit and nigrostriatal pathway with significant correlation of TRODAT-1 binding ratio. In this study, 12 CO patients exhibited symptoms of Parkinsonism. These results further indicate that CO-induced early WM injuries in dopaminergic pathways led to dopamine transporter dysfunction of the striatum and symptoms of Parkinsonism observed in CO patients.

This study has some limitations that are worth noting. First, the patient number was small, so further study on a larger population is warranted. Second, the DKI data were acquired with only three high b-values. A higher number of b-values would help minimize fitting errors in the DKI estimation [28, 29]. However, in these conditions the concomitant lengthening of scan time may increase the number of motion artefacts in the dataset [30]. Third, the TRODAT-1 SPECT scan was not performed in the control group, so whether or not the TRODAT-1 binding ratios were significantly lower in CO patients in comparison with healthy controls cannot be deduced from this study. Finally, the Tc-99m-TRODAT-1 SPECT scan and DKI acquisition were not performed on the same day. Although the time difference between the two scans was <1 week, the correlation analysis may have been affected due to this timing discrepancy.

Conclusions

In the present study we performed both DKI and Tc-99m-TRODAT-1 SPECT to reveal, respectively, WM injuries and

dysfunction of dopamine transporter in patients with acute CO intoxication. The voxel-wise analysis showed that patients with acute CO intoxication exhibited widespread WM alterations in both supra- and infra-tentorial regions. The correlation analysis demonstrated significant correlations between DKI indices and T_{onset}, T_{coma}, COHb% and TRODAT-1 binding ratios in multiple injured WM regions. Therefore, we conclude that DKI and Tc-99m TRODAT-1 SPECT were helpful in investigating global WM injuries associated with dopamine transporter dysfunctions of the striatum in patients with acute CO intoxication.

Funding This study received funding by Dr. Ping-Hong Lai and Dr. Ming-Chung Chou from Ministry of Science and Technology (MOST) of Taiwan (106-2314-B-075B-002 -MY3 and 101-2314-B-037-047-MY2) and Dr. Jie-Yuan Li from Veterans General Hospitals and University System of Taiwan Joint Research Program (VGHUST100-G3-2-3).

Compliance with ethical standards

Guarantor The scientific guarantor of this publication is Dr. Jie-Yuan Li.

Conflict of interest The authors of this manuscript declare no relationships with any companies whose products or services may be related to the subject matter of the article.

Statistics and biometry No complex statistical methods were necessary for this paper.

Informed consent Written informed consent was obtained from all subjects (patients) in this study.

Ethical approval Institutional Review Board approval was obtained.

Methodology
- Prospective
- Case-control study
- Performed at one institution

References

1. Gale SD, Hopkins RO, Weaver LK, Bigler ED, Booth EJ, Blatter DD (1999) MRI, quantitative MRI, SPECT, and neuropsychological findings following carbon monoxide poisoning. Brain Inj 13: 229–243
2. Prockop LD (2005) Carbon monoxide brain toxicity: Clinical, magnetic resonance imaging, magnetic resonance spectroscopy, and neuropsychological effects in 9 people. J Neuroimaging 15:144–149
3. Weaver LK, Hopkins RO, Chan KJ et al (2002) Hyperbaric oxygen for acute carbon monoxide poisoning. N Engl J Med 347:1057–1067
4. Chiew AL, Buckley NA (2014) Carbon monoxide poisoning in the 21st century. Crit Care (2014) 18:221
5. Neil J, Miller J, Mukherjee P, Hüppi PS (2002) Diffusion tensor imaging of normal and injured developing human brain - a technical review. NMR Biomed 15:543–552
6. Chang CC, Chang WN, Lui CC et al (2011) Clinical significance of the pallidoreticular pathway in patients with carbon monoxide intoxication. Brain 134:3632–3646
7. Chang CC, Chang WN, Lui CC et al (2010) Longitudinal study of carbon monoxide intoxication by diffusion tensor imaging with neurospsychiatric correlation. J Psychiatry Neurosci 35:115–125
8. Lin WC, Lu CH, Lee YC et al (2009) White Matter Damage in Carbon Monoxide Intoxication Assessed in Vivo Using Diffusion Tensor MR Imaging. AJNR Am J Neuroradiol 30:1248–1255
9. Chang CC, Lee YC, Chang WN et al (2009) Damage of White Matter Tract Correlated with Neuropsychological Deficits in Carbon Monoxide Intoxication after Hyperbaric Oxygen Therapy. J Neurotrauma 26:1263–1270
10. Arab A, Wojna-Pelczar A, Khairnar A, Szabó N, Ruda-Kucerova J (2018) Principles of diffusion kurtosis imaging and its role in early diagnosis of neurodegenerative disorders. Brain Res Bull 139:91–98
11. Tsai PH, Chou MC, Chiang SW et al (2017) Early white matter injuries in patients with acute carbon monoxide intoxication A tract-specific diffusion kurtosis imaging study and STROBE compliant article. Medicine (Baltimore) 96
12. Kinoshita T, Sugihara S, Matsusue E, Fujii S, Ametani M, Ogawa T (2005) Pallidoreticular damage in acute carbon monoxide poisoning: Diffusion-weighted MR imaging findings. AJNR Am J Neuroradiol 26:1845–1848
13. O'Donnell P, Buxton PJ, Pitkin A, Jarvis LJ (2000) The magnetic resonance imaging appearances of the brain in acute carbon monoxide poisoning. Clin Radiol 55:273–280
14. Kao HW, Cho NY, Hsueh CJ et al (2012) Delayed Parkinsonism after CO Intoxication: Evaluation of the Substantia Nigra with Inversion-Recovery MR Imaging. Radiology 265:215–221
15. Huang WS, Lin SZ, Lin JC, Wey SP, Ting G, Liu RS (2001) Evaluation of early-stage Parkinson's disease with Tc-99m-TRODAT-1 imaging. J Nucl Med 42:1303–1308
16. Jenkinson M, Bannister P, Brady M, Smith S (2002) Improved optimization for the robust and accurate linear registration and motion correction of brain images. Neuroimage 17:825–841
17. Smith SM (2002) Fast robust automated brain extraction. Hum Brain Map 17:143–155
18. Mori S, Oishi K, Jiang H et al (2008) Stereotaxic white matter atlas based on diffusion tensor imaging in an ICBM template. Neuroimage 40:570–582
19. Vercauteren T, Pennec X, Perchant A, Ayache N (2009) Diffeomorphic demons: Efficient non-parametric image registration. Neuroimage 45:S61–S72
20. Beppu T, Fujiwara S, Nishimoto H et al (2012) Fractional anisotropy in the centrum semiovale as a quantitative indicator of cerebral white matter damage in the subacute phase in patients with carbon monoxide poisoning: correlation with the concentration of myelin basic protein in cerebrospinal fluid. J Neurol 259:1698–1705
21. Hou X, Ma L, Wu L et al (2013) Diffusion Tensor Imaging for Predicting the Clinical Outcome of Delayed Encephalopathy of Acute Carbon Monoxide Poisoning. Eur Neurol 69:275–280
22. Lo CP, Chen SY, Chou MC et al (2007) Diffusion-tensor MR imaging for evaluation of the efficacy of hyperbaric oxygen therapy in patients with delayed neuropsychiatric syndrome caused by carbon monoxide inhalation. Eur J Neurol 14:777–782
23. Parvizi J, Damasio A (2001) Consciousness and the brainstem. Cognition 79:135–160
24. Song SK, Yoshino J, Le TQ et al (2005) Demyelination increases radial diffusivity in corpus callosum of mouse brain. Neuroimage 26:132–140
25. Wheeler-Kingshott CA, Cercignani M (2009) About "Axial" and "Radial" Diffusivities. Magn Reson Med 61:1255–1260
26. Thom SR (1990) Carbon Monoxide-Mediated Brain Lipid-Peroxidation in the Rat. J Appl Physiol 68:997–1003

27. Thom SR, Bhopale VM, Han ST, Clark JM, Hardy KR (2006) Intravascular neutrophil activation due to carbon monoxide poisoning. Am J Respir Crit Care Med 174:1239–1248
28. Chou MC, Ko CW, Chiu YH, Chung HW, Lai PH (2017) Effects of B Value on Quantification of Rapid Diffusion Kurtosis Imaging in Normal and Acute Ischemic Brain Tissues. J Comput Assist Tomogr 41:868–876
29. Yan X, Zhou MX, Ying LF et al (2013) Evaluation of optimized b-value sampling schemas for diffusion kurtosis imaging with an application to stroke patient data. Comput Med Imaging Graph 37:272–280
30. Li X, Yang J, Gao J et al (2014) A robust post-processing workflow for datasets with motion artifacts in diffusion kurtosis imaging. PLoS One 9:e94592